Probing the Nature of Acetylene Bound to the Active Site of a NiNa−Zeolite Y Catalyst by in situ Neutron Scattering

John F. C. Turner,[†] Chris J. Benmore,[‡] Carolyn M. Barker,[†] Nikolas Kaltsoyannis,[§] John Meurig Thomas,[†] William I. F. David,[‡] and C. Richard A. Catlow*,[†]

The Royal Institution of Great Britain, 21 Albemarle Street, London W1X 4BS, U.K., ISIS Facility, Rutherford Appleton Laboratory, Chilton, Oxon OX11 OQX, U.K., and Centre of Theoretical and Computational Chemistry, University College London, Gower Street, London WC1E 6BT, U.K.

Received: May 16, 2000

An investigation of the interaction between a catalytic system and its substrate (reactant) using neutron diffraction with isotopic substitution (NDIS) is reported. Specifically, the interaction between acetylene and nickel ion exchanged sodium zeolite Y has been investigated using NDIS in situ, revealing the radial distribution of distances at the disordered nickel sites. This is the first time that NDIS has been used for an in situ study, as well as the first time that a catalytic system has been structurally interrogated using this method. The experimental findings are supported and amplified by density functional calculations. Both experiment and theory reveal a $Ni^{II}-(\eta^2-C_2H_2)$ complex with small but significant deviation of the geometry exhibited by acetylene in its free state.

Introduction

Nickel ion exchanged zeolite Y is an efficient catalyst for the cyclotrimerization of acetylene to benzene at temperatures below 100 °C.[1,2] In their as-prepared state, such catalysts have typical composition $Ni_{X/2}Na_{59-X}Al_{59}Si_{133}O_{384}$ and are henceforth designated NiNaY. The Ni^{II} ions are located predominantly at the so-called S_I sites (i.e., at the center of the double six rings of the faujasite structure), but it has been convincingly shown by time-resolved in situ X-ray diffraction studies[3−5] that a substantial fraction of these ions migrate during "activation" in acetylene and that they subsequently take up extraframework sites such as the S_{II} and S_I, where they become catalytically active in cyclotrimerization.[6,7]

Although a combination of X-ray diffraction (using the Rietveld method of data analysis)[3−5] and X-ray absorption spectroscopy[4,5] has been used to give detailed and quantitative information about the heavy atom positions in these catalysts, no technique with special sensitivity to light atoms has hitherto been used. Light atoms in this context signify those with low Z — in this study, hydrogen. This paper describes the first in situ structural interrogation of the nickel ion sites in NiNaY in the dehydrated and activated forms using neutron diffraction with isotopic substitution.

Previous neutron-based studies[8−10] have been very successful in locating the sites of adsorbed species within microporous heterogeneous catalysts. The method used for those studies (of e.g., bound xenon in zeolite ρ,[8] of d^5-pyridine in gallozeolite-L,[9] and of benzene in zeolite Y[10]) was based on Rietveld analysis of the powder diffraction profile. For these relatively straightforward studies, restricted to investigations at temperatures not higher than 210 K, powder diffraction procedures were suitable, just as they were for X-ray powder refinement studies of NiNaY model catalysts at elevated temperatures. Here the coordination of d_2-acetylene to Ni in NiNaY is determined by a diffraction experiment which gives purely the local structure about the Ni sites. Specifically, substitution of nickel of normal isotopic abundance, subsequentially written as ^{Nat}Ni, by the stable isotope ^{62}Ni allows the large difference in bound elastic scattering length, b, between the two isotopes to be exploited ($b(^{Nat}Ni) = 10.3$ fm and $b(^{62}Ni) = -8.7$ fm). Other isotopes and their scattering lengths relevant to this work can be found in the literature.[11] These results illustrate well the application of neutron scattering to spatially distributed atoms with low site occupancies in a crystalline system, using isotopic labeling and measurement of the total structure factor. The interpretation of the structural properties revealed by the neutron data is assisted by density functional theory (DFT) calculations on the Ni^{2+}−acetylene system.

Theory

The quantity measured in this experiment is the differential neutron scattering cross section, $\partial\sigma/\partial\Omega$, of which the interference part (or total structure factor) can be expressed as a linear sum of the partial structure factors, S(Q). The structure factor describes the spatial distribution of scattering centers (in this case atomic nuclei) of the sample in question. Thus in the total structure factor, all distances between all scatterers are present, weighted according to the concentration of each particular type of atom, c, and their scattering length, b. The differential neutron scattering cross section can be written as

$$\frac{\partial\sigma}{\partial\Omega} = N\left\{\sum_{\alpha} c_\alpha b_\alpha^2 + \sum_{\beta} c_\alpha b_\alpha c_\beta b_\beta [S_{\alpha\beta}(Q) - 1]\right\} \qquad (1)$$

where the partial structure factor $S_{\alpha\beta}(Q)$ describes interactions between atoms of type α and β. $S_{\alpha\beta}(Q)$ in turn is related directly to its real space radial distribution function $g_{\alpha\beta}(r)$ through Fourier transformation.[12]

By performing neutron diffraction experiments on two samples which are identical in every respect except that a

* Corresponding author.
[†] The Royal Institution of Great Britain.
[‡] ISIS Facility.
[§] Centre of Theoretical and Computational Chemistry.

10.1021/jp0017994 CCC: $19.00
Published on Web 07/21/2000

specific atom has been isotopically enriched, it is in principle possible to extract correlations involving just the isotopically enriched species (in this work Ni). This is the basis of the neutron diffraction with isotopic substitution (NDIS) technique.[12,13] Previously, this method has been applied to disordered systems such as liquids and glasses, but it is shown here that it is equally applicable to spatially distributed atoms with low site occupancies in crystalline systems.

Methodology

^{Nat}NiNaY and ^{62}NiNaY at 6% w/w were prepared according to standard literature procedures.[4,5] $^{62}NiC1_2 \cdot 6H_2O$ was synthesized by dissolving ^{62}Ni in 10% hydrochloric acid and evaporating the solution. The solution was dissolved in 200 mL of distilled water, and NaY (Al/Si 1:2.52) was added as a fine powder. The slurry was stirred overnight and then filtered and washed with water several times, the supernatant being retained for subsequent recovery of the ^{62}Ni as the hydroxide. Deuteration of the powder was effected by slurrying the NiNaY in D_2O (50 mL) under a N_2 atmosphere for 3 h and then evaporating the solvent to yield a damp cake of material. This process was repeated twice, yielding a product which contained no hydrogen.

The synthesis for ^{Nat}NiNaY was performed identically, substituting recrystallized $NiCl_2 \cdot 6H_2O$ for the isotopically labeled quantity. Perdeuteracetylene was prepared on a high vacuum line by the reaction between D_2O and CaC_2 followed by purification by multiple cryogenic transfers. Purity was assessed by FTIR spectroscopy in the gas phase and it was found that the deuterium was ~100%.

A series of neutron diffraction measurements was performed on the two samples, with and without the addition of deuterated acetylene, using the SANDALS diffractometer at the ISIS pulsed neutron facility. The zeolite powder samples were contained in flat-plate 2 mm internal thickness titanium−zirconium containers of wall thickness 1 mm (each) with a gold O-ring seal. Dehydration was effected by evacuation to 10^{-6}mbar at 300 °C until the scattered neutron intensity fell to a constant quantity. Simultaneously, d_2-acetylene was barometrically measured into a constant volume bulb such that 3 molar equivalents based on the Ni concentration in the sample were contained therein.[14] After data acquisition on the evacuated and dehydrated sample was completed, the sample was exposed to this known amount of d_2-acetylene and data were collected once the scattering intensity was constant again. This was very rapid (~15 s) on the time scale of the data collection (8 h). This procedure was repeated using identical masses and volumes of material on the other isotopically labeled sample.

Data Analysis

The neutron diffraction data were analyzed using the ATLAS package[15] which corrects for background, attenuation, and multiple scattering effects. For powdered samples with an associated packing fraction it is necessary to apply these corrections in an iterative manner until the differential neutron cross section tends to the correct high momentum transfer limit.[13] The data were normalized using a flat plate 3.5 mm thick vanadium slab to determine the absolute scattering. The Q space data were truncated at $Q = 30\text{Å}^{-1}$ and Fourier transformed into real space using a window function to reduce spurious transform artifacts. Unphysical distances, i.e., those less than 0.75 Å were discarded.

The dehydrated sample measured in this experiment had the composition $Ni_XNa_{59-X}Al_{59}Si_{133}O_{384}$ and an atomic number density of 0.04276 atoms Å^{-3}. Similarly, the sample sorbed with acetylene had a composition of NaNiY + $C_{27.28}D_{27.28}$. The neutron total radial distribution function for ^{Nat}NiNaY sample with acetylene added, $G_{NiNaY+C2D2}(r)$, can be written as a linear weighted combination of NiNaY−NiNaY, acetylene−NiNaY, and acetylene−acetylene contributions (where $A_{subscript}$ is the neutron weighting factor), i.e.,

$$G_{NiNaY+C2D2}(r) = A_1 G_{NiNaY-NiNaY}(r) + A_2 G_{NiNaY-C2D2}(r) + A_3 G_{C2D2-C2D2}(r) \quad (2)$$

Thus it follows that the environment of the Ni atoms, described by the $\Delta G_{Ni}(r)$ difference functions for the dehydrated and acetylene samples may be expressed as

$$\Delta G_{NiX}^{\text{dehydrated}}(r) = A_4 G_{Ni-NiNaY}(r)$$
$$= 0.720 g_{NiO}(r) + 0.184 g_{NiSi}(r) + 0.061 g_{NiAl}(r) + 0.031 g_{NiNa}(r) + 0.004 g_{NiNi}(r) \quad (3)$$

$$1.185 \times \Delta G_{NiX}^{C2D2}(r) = A_4 G_{NiNiNaY}(r) + A_5 G_{Ni-C2D2}(r)$$
$$= 0.720 g_{NiO}(r) + 0.184 g_{NiSi}(r) + 0.061 g_{NiAl}(r) + 0.031 g_{NiNa}(r) + 0.004 g_{NiNi}(r) + 0.062 g_{NiC}(r) + 0.062 g_{NiD}(r) \quad (4)$$

From these equations it becomes clear that, by scaling the acetylene sorbed sample NiNaY + $C_{27.28}D_{27.28}$ by a factor of 1.185, the same weighting factors appear on the Ni−NiNaY contributions. As such, the difference between $[1.185\Delta G_{NiX}^{C2D2}(r)] - [\Delta G_{NiX}^{\text{dehydrated}}(r)]$ will be due to correlations between the Ni−acetylene plus any changes in the environment of the Ni atoms with respect to the zeolite Y structure due to Ni migration.

Computational Methodology

Density functional theory, as implemented in the code Dmol,[16] was used to calculate the geometries of Ni^{II}, C_2H_2, and $Ni^{II}-(\eta^2-C_2H_2)$. Both local density and gradient corrected calculations were performed; in particular we employed the local potential energy functional of Vosko, Wilk, and Nusair (VWN)[17] and the Becke[18] nonlocal exchange with the Lee, Yang, and Parr[19] nonlocal correlation correction (BLYP). BLYP was used because it was found to reproduce most accurately the second ionization potential of nickel, compared with the nonlocal functionals of Perdew and Wang (PW91)[20] and BPW91.[18,20] All calculations used a double numerical basis set with polarization functions on all atoms (DNP). No symmetry constraints were used when modeling the $Ni^{II}-(\eta^2-C_2H_2)$ complex to prevent unrealistic restriction of the molecular geometry. The initial approximate geometry for the $Ni^{II}-(\eta^2-C_2H_2)$ complex was found by molecular mechanics methods embedded within MSI's Discover3.0 code.[21] A spin unrestricted wave function was employed in modeling the $Ni^{2+}(^3F)$ ground state.

Results and Discussion

Our experiments are based on the measurement of the total differential neutron cross section for each sample. Typical data are shown in Figure 1, where the changes in Bragg diffraction (elastic coherent scattering signal) are clearly seen upon nickel isotope substitution. The differences between the ^{Nat}NiNaY and ^{62}NiNaY samples with and without d_2-acetylene are shown in Figure 2 with the corresponding error bars. However, it is more

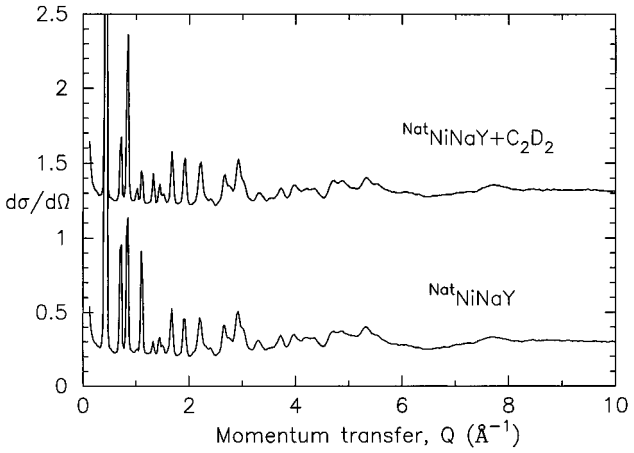

Figure 1. Measured differential neutron cross sections for dehydrated zeolite (NiNaY) and zeolite with acetylene (NiNaY + C_2D_2) in absolute units of barns/atom/steradian shown out only to $Q = 10$ Å^{-1}. The spectra show significant differences in the measured neutron diffraction pattern.

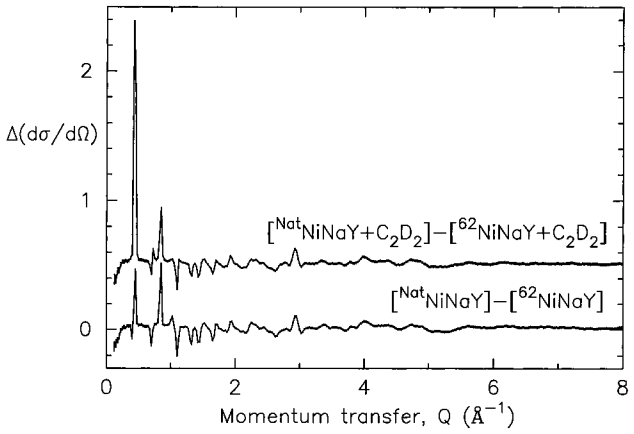

Figure 2. Measured first-order neutron difference functions ^{Nat}NiNaY−^{62}NiNaY with and without acetylene present, with error bars. The acetylene curve has been displaced by 0.5.

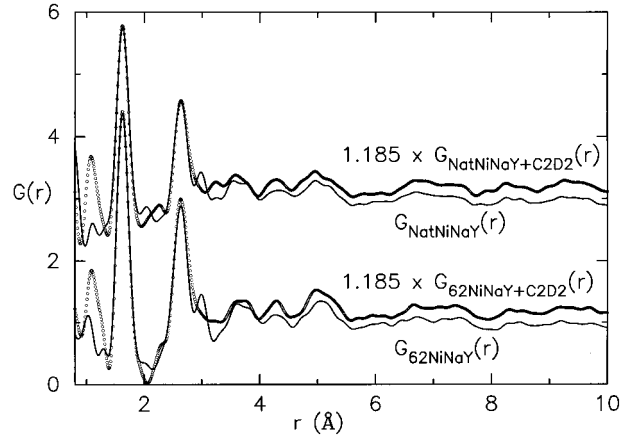

Figure 3. Measured radial distribution functions for four NiNaY samples, obtained by Fourier transformation of the Q space data sets shown in Figure 1 truncated at 30 Å^{-1}. The solid line represents the dehydrated zeolite samples and the circles are the zeolite plus acetylene samples (scaled by a factor of 1.185 to give the same weighting factors as for the dehydrated zeolite function, see text).

useful to interpret these data in real space as shown in Figure 3. In this figure the NiNaY + C_2D_2 difference has been scaled by a factor of 1.185 such that it has the same neutron weighting factors that appear in the dehydrated NiNaY difference function

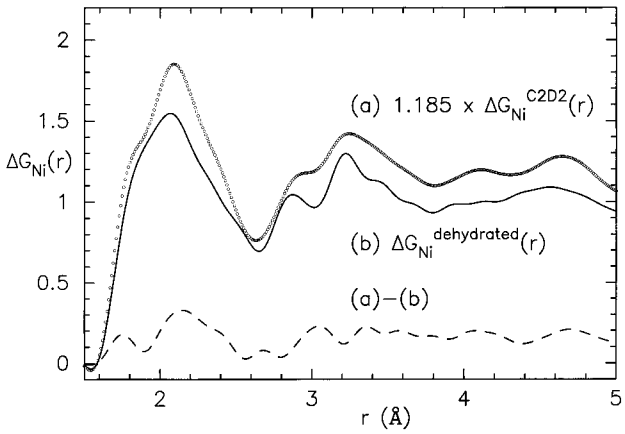

Figure 4. Real space Ni environment in NiNaY, measured with (circles), and without (solid line) the presence of acetylene (the NiNaY + C_2D_2 difference has been scaled by a factor of 1.185, see text).

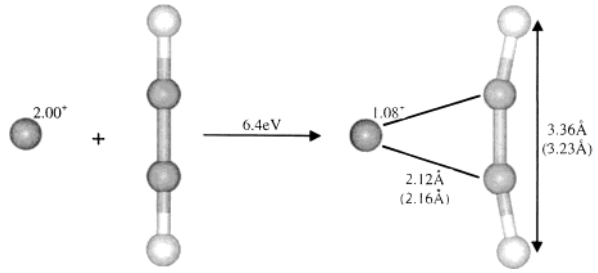

Figure 5. BLYP/DNP optimized geometries, Ni charge, and binding energy for the interaction of one molecule of acetylene with a bare Ni^{II} ion. Distances obtained from neutron scattering data in brackets.

(see eqs 3 and 4). In this representation there are clear differences between the ^{Nat}Ni and ^{62}Ni dehydrated samples related to the difference in scattering of the substituted Ni atoms. Upon the addition of acetylene, the intramolecular acetylene C−C and C−D bond lengths are clearly observed around $r_{CC} = 1.16 \pm 0.01$ Å and $r_{CD} = 2.3 \pm 0.05$ Å. While the structure of the NiNaY is largely unchanged with the acetylene present, there are small structural rearrangements about 2.0 Å and in the 3.0 Å region, which is more evident in Figure 4 where the Ni environments with and without acetylene yield peaks at 2.09 ± 0.02 Å (with a low *r* shoulder at 1.86 ± 0.03 Å) and 2.88 ± 0.02 Å. On the basis of previous EXAFS studies[4] of dehydrated $Ni_{59}Al_{59}Si_{133}O_{384}$ (denoted NiY) these correlations are assigned predominantly to Ni−O correlations. Integrating under the dehydrated-Ni neutron difference curve out to 3.0 Å, assuming only Ni−O correlations, we find an average coordination of 3.6(1) oxygen atoms surrounding a Ni atom in NiNaY, which is in contrast to the EXAFS results on NiY which find a Ni−O coordination number of 8 over approximately the same range.[4] However, the peak at 3.24 ± 0.02 Å corresponds to known Ni−Si and Ni−Al distances.

To assist the interpretation of the data, theoretical techniques were employed to calculate the structure of a model system. Using density functional theory (DFT), the interaction between Ni^{2+} and acetylene was investigated. The BLYP/DNP calculated geometries for the interaction of a bare Ni^{2+} ion with one molecule of acetylene are shown in Figure 5. The optimized geometry was found to be of C_{2v} symmetry, i.e., the Ni ion is equidistant from each carbon and each hydrogen atom; deviation from the midpoint of the C−C vector, the "off-centered" geometry was found to be of higher energy. Upon interaction of the acetylene with the Ni^{2+} ion there is substantial deformation of the organic moiety. The C−C triple bond elongates from

TABLE 1: Bond Lengths (in Å) and Angles (in degrees) of Acetylene Unbound and Bound to Ni^{II} as Calculated by the BLYP Nonlocal Density Functional and *VWN Local Density Functional

	C−C	C−H	H−H	Ni−C	Ni−H	C−C−H
C_2H_2	1.21	1.07	3.36			180.0
	1.21	1.08*	3.35*			180.0*
$Ni^{II}-$	1.26	1.10	3.44	2.12	2.81	169.0
$\eta^2(C_2H_2)$	1.25	1.11*	3.42	2.05*	2.76*	169.4*

1.21 Å to 1.26 Å; the C−H bonds bend back away from the metal center by 11°. The distances and angles are shown in Table 1. The effective Mulliken charge on the nickel ion is reduced from +2.00 to +1.08 due to donation of electron density from the acetylene C−C triple bond.

The gradient corrected binding energy for the $Ni^{II}-(\eta^2-C_2H_2)$ complex was calculated to be 6.4 eV, which is lower than the value of 8.1 eV determined by the local VWN density functional. This difference is primarily due to the overestimation of electron correlation by the local density method, producing shorter Ni−C and Ni−H bond lengths. However, even though the VWN functional overbinds the $Ni^{II}-(\eta^2-C_2H_2)$, examination of Table 1 shows there to be excellent agreement between nonlocal and local functionals in calculating the geometry of coordinated acetylene ligand. Although the model is relatively crude chemically, it may be expected that the structural features will not be grossly different from the experimentally measured values. More detailed calculations are currently in progress involving the zeolite host explicitly.

The double difference curve $1.185\Delta G_{Ni}^{C2D2}(r) - \Delta G_{Ni}^{dehydrated}(r)$ shown by the dashed line in Figure 4 has peaks at 1.76 ± 0.01 Å, 2.16 ± 0.02 Å and 3.05 ± 0.02 Å. This difference contains contributions from Ni−acetylene correlations as well as changes in the Ni−NiNaY environment with the addition of acetylene. The latter two distances compare favorably with the calculated DFT distances of the $Ni^{II}-(\eta^2-C_2H_2)$ complex distances in Table 1; see also Figure 5. However, the migration of Ni ions within the zeolitic host is a well-known experimental fact,[2,3] and migration from the S_I site may be expected on treatment with d_2-acetylene. As the neutron difference functions are extremely sensitive to small changes in the Ni−O environment (see weighting factors on eqs 3 and 4), a more quantitative analysis of the $Ni^{II}-(\eta^2-C_2H_2)$ complex is not possible without taking the Ni migration into account. Qualitatively, however, the neutron data is consistent with structural features of the predicted Ni complex associated with the Dewar−Chatt−Duncanson model for π acid coordination. This model explains the structural changes in terms of a σ-base donation to the metal and a synergystic π-acid interaction metal to hydrocarbon. These factors necessarily occur together and the predominance of one over the other will depend on symmetry, energy match, metal electron count, and overlap. In this case, Ni^{II} will act as a Lewis acid more than a good π-base with an associated reduction in charge of the Ni ion and concomitant structural changes in the coordination complex formed between Ni and NiNaY. However, additional modeling techniques and/or experiments will be required to separate out explicitly the $Ni^{II}-(\eta^2-C_2H_2)$ complex formation from changes in the Ni−O migration observed in the NDIS data presented in this study.

Acknowledgment. This work was funded under the auspices of the grant GR/L 13834 from the EPSRC, whom we thank for funding. We also thank Dr. Allan Pashkovski, Managing Director, JV Isoflex (Moscow) for provision of 99% purity ^{62}Ni. Dr. G. Sankar (RI) for fruitful discussions and help with the preparation of the NiNaY samples, and Dr. G. S. M. McGrady (King's College London) for help in preparation of the d_2-acetylene.

References and Notes

(1) Pichat, P.; Vedine, J. C.; Gallezot, P.; Imlich, B. *J. Catal.* **1974**, *32*, 190.
(2) Maddox, P. J.; Stachurski, J.; Thomas, J. M. *Catal. Lett.* **1988**, *1*, 191.
(3) Couves, J. W.; Jones, R. H.; Thomas, J. M.; Smith, B. J. *Adv. Mater.* **1990**, *2*, 181.
(4) Dooryhee, E.; Maddox, P. J.; Steel, A.; Catlow, C. R. A.; Couves, J. W.; Townsend, R. P.; Thomas, J. M. *Faraday Discuss.* **1990**, 89.
(5) Dooryhee, E.; Catlow, C. R. A.; Couves, J. W.; Maddox, P. J.; Thomas, I. M.; Greaves, G. N.; Steel, A. T.; Townsend, R. P. *J. Phys. Chem.* **1991**, *95* (1), 4514.
(6) George, A. R.; Catlow, C. R. A.; Thomas, J. M. *Catal. Lett.* **1991**, *8*, 193.
(7) George, A. R.; Catlow, C. R. A.; Thomas, J. M. *J. Chem. Soc., Faraday Trans.* **1995**, *91*, 3975.
(8) Wright, P. A.; Thomas, J. M.; Ramdas, S. *J. Chem. Soc., Chem. Commun.* **1984**, 1338.
(9) Wright, P. A.; Thomas, J. M.; Cheetham, A. K.; Nowak, A. K. *Nature* **1985**, *318*, 611.
(10) Fitch, A. N.; Jobic, H.; Renouprez, A. *J. Phys. Chem.* **1986**, *90*, 1311.
(11) Sears, V. F.; *Thermal Neutron Scattering Lengths and Cross Sections for Condensed Matter Research*; AECL Report 8490, 1984.
(12) Finney, J. L.; Soper, A. K. *Chem. Soc. Rev.* **1994**, *23*, 1, 1. Enderby, J. E.; *Chem. Soc. Rev.* **1995**, *24* (3), 159 and references therein.
(13) Benmore, C. J.; Salmon, P. S. *Phys. Rev. Lett.* **1994**, *73* (2), 264.
(14) Turner, J. F. C.; Done, R.; Dreyer, J.; David, W. I. F.; Catlow, C. R. A. *Rev. Sci. Instrum.* **1999**, 70 (5), 2325.
(15) Soper, A. K.; Howells, W. S.; Hannon, A. C. *Analysis of Time-of-Flight Diffraction Data from Liquid and Amorphous Samples*; RAL report 98-046 1989.
(16) DMOL3.8, Molecular Simulations Inc.: San Diego, CA (1998).
(17) Vosko, S.; Wilk, L.; Nusair, W. *Can. J. Phys.* **1980**, *58*, 1200.
(18) Becke, A. *Phys. Rev. A* **1988**, *38*, 3098.
(19) Lee, C.; Yang, W.; Parr, R. *Chem. Phys. Lett.* **1997**, *265*, 115.
(20) Perdew, J. P.; Wang, Y. *Phys. Rev.* 1992, B45, 13244.
(21) Discover 3.0, Molecular Simulations Inc.: San Diego, CA, 1995.